Int J Clin Exp Med 2021;14(6):1971-1982
www.ijcem.com /ISSN:1940-5901/IJCEM0111739

Original Article

Derlin-1 protects alveolar epithelial cells against endoplasmic reticulum stress-induced apoptosis

Yin-Hui Sun[1*], Shuang-Xiang Tan[2*], Rui-Cheng Hu[1], Yan Peng[1], Wen-Qiong Chen[1], Li-Huai Wang[3], Ai-Guo Dai[2], Li-Le Wang[1]

[1]Department of Respiratory Medicine, Hunan Provincial People's Hospital/The First Affiliated Hospital of Hunan Normal University, Changsha, China; [2]Hunan Province Institute of Gerontology, Hunan Provincial People's Hospital/The First Affiliated Hospital of Hunan Normal University, Changsha, China; [3]Department of Oncology, The First Hospital of Hunan University of Chinese Medicine, Changsha, China. [*]Equal contributors.

Received April 1, 2020; Accepted December 26, 2020; Epub June 15, 2021; Published June 30, 2021

Abstract: This study explores the function of Derlin-1 expression in the lungs of cigarette smoke-exposed, chronic obstructive pulmonary disease (COPD) rats, and investigates whether Derlin-1 reduces the apoptosis of RLE-6TN cells induced by cigarette smoke extract (CSE) through the activation of an endoplasmic reticulum-associated degradation mechanism. A COPD rat model was generated by exposure to passive smoking. Hematoxylin and eosin staining was used to determine the pathologic changes in the lungs, and the expression and distribution of Derlin-1 in the lung tissue were measured using immunohistochemistry. The Derlin-1 gene was knocked down using small interfering RNA (siRNA) in the RLE-6TN alveolar epithelial cell line or over-expressed using lentiviral transfection. The cell apoptotic rate was measured using flow cytometry. Lung structure destruction and obstructive pulmonary ventilation function impairment were measured in the cigarette smoke-exposed COPD rats. The Derlin-1 mRNA and protein expressions were significantly up-regulated in the rats' lungs after two months of smoke exposure and moderately decreased after four months of smoke exposure. CSE treatment up-regulated the expression of Derlin-1 mRNA and protein in RLE-6TN cells. The knockdown of Derlin-1 decreased the IRE1 protein expression, increased the expressions of CHOP and the p-JNK protein, and increased the apoptotic rate in the RLE-6TN cells. The over-expression of Derlin-1 led to an increased expression of IRE1, decreased CHOP and p-JNK expressions, and a reduced apoptotic rate. The results show that cigarette smoke promotes alveolar epithelial cell apoptosis via an ERS mechanism, and Derlin-1 plays a key role in protecting alveolar epithelial cells from the apoptosis induced by cigarette smoke.

Keywords: Derlin-1, apoptosis, chronic obstructive pulmonary disease, RLE-6TN cells, cigarette smoke, endoplasmic reticulum stress

Introduction

Smoking is a major risk factors for chronic obstructive pulmonary disease (COPD) [22]. An increasing amount of evidence shows that the harmful components in cigarette smoke can induce endoplasmic reticulum stress (ERS) in lung tissue cells [8, 25]. One study confirmed that over-activation induces apoptosis in COPD patients' pulmonary cells, causing pulmonary structural damage, accelerated lung injury, and pulmonary hypofunction, thereby promoting the development of COPD [14]. The expressions of endoplasmic reticulum (ER) chaperone and ER-associated protein degradation (ERAD) proteins play essential roles in ER cells by providing protection against the deleterious effects of ERS [9]. Recently, an antiporter, Derlin-1, was shown to attenuate ERS. Derlin-1, a homologue of Der1 found in the endoplasmic reticulum membrane, is involved in the transport of misfolded proteins across the endoplasmic reticulum [12, 26]. Many studies have shown that a loss of Derlin-1 is involved in several diseases, such as Parkinson's disease, amyotrophic lateral sclerosis, cystic fibrosis, etc., but the over-expression of Derlin-1 promotes resistance to ERS-induced apoptosis and the invasion of lung cancer, colon cancer, bladder cancer, and squamous cell carcinoma [4, 5, 17, 20]. Although Derlin-1 plays different roles in different diseases, it is evident that

Table 1. siRNA target gene sequence

Target gene	Target Sequence	Start pos	GC%
siRNA1	GGCCAGCAGACTATTTATT	327	42.11%
siRAN2	CTGGCTTAGCCATGGATAT	381	47.37%
siRNA3	TGAGCTCATTGGAAACCTT	562	42.11%

Derlin-1 participates in ERAD and mitigates the accumulation of toxic proteins, thereby relieving ERS. No previous studies have indicated whether Derlin-1 plays a role in COPD. The current study was done as a preliminary investigation into the role of Derlin-1 in smoking-induced COPD. Our findings will help to elucidate the potential mechanism of Derlin-1 induced ERS in smoking-induced COPD.

Materials and methods

Animals and cell lines

Forty, 10-week-old, clean-grade, male Sprague-Dawley (SD) rats weighing 200±20 g were purchased from the Department of Laboratory Animals of Central South University (License key: SCXK [Xiang] 2009-0004).

RLE-6TN cells were obtained from the American Type Culture Collection (Manassas, VA) (strain F344, *Rattus norvegicus*) and cultured in a Dulbecco's modified Eagle's medium-F12 medium (Gibco, Grand Island, NY) containing 2 mmol/L of glutamine, 100 U/mL of penicillin, l00 μg/mL of streptomycin, 200 pg/mL of keratinocyte growth factor, and 10% fetal bovine serum (Gibco).

Alveolar type II epithelial cells (AT-II) were isolated, purified, and cultured. Alkaline phosphatase and surfactant protein A staining were used for identification.

Preparation of CSE

Cigarettes (Furong Wang, China Tobacco Hunan Industrial Corporation, Hunan, China) were used to prepare CSE as previously reported [21]. The concentration of the cigarettes was set according to pre-laboratory testing. We used a syringe to inject the smoke (35 mL) into a glass bottle containing 5 mL of phosphate-buffered saline through a three-way tube. This step was repeated 10 times at 1-min intervals for 2 s at a time. The pH of the resulting mixture was adjusted to 7.4. The mixed liquor of filtrate was 100% CSE, which was diluted to 10% CSE. The shelf life of the 10% CSE was 30 min.

Establishment of the COPD model

We divided the rats randomly into four groups with 10 rats in each group: the control group, smoking group 1 (exposure to passive smoking for 2 months), smoking group 2 (exposure to passive smoking for 4 months), and the smoking cessation group (exposure to passive smoking for 4 months followed by smoking cessation for 1 month). The rats were exposed to the smoke of 10 cigarettes twice a day (1 h each time) in a custom-built exposure box (50 cm × 50 cm × 35 cm) with at least 4 h between exposures [6].

Pulmonary function testing

The rats were anesthetized using 10% chloral hydrate (3 mL/kg) using an intraperitoneal injection. The tidal volume was set at 10 mL/kg, and the respiratory rate was 60 breaths per minute. After a period of calm breathing, the syringe was filled with a volume of gas equivalent to the tidal volume amount through the three-way tube at the end of the expiration, then immediately turned off. Negative pressure (-25 cm H_2O) was connected for air exhaust, causing deep expiration. The volume change was calculated by a microcomputer (Medlab-U/4C; Nanjing Medease Science and Technology Co., Ltd., Nanjing, China) for the first 0.3 s of the forced expiratory volume (FEV 0.3), forced vital capacity (FVC), and peak expiratory flow (PEF).

Hematoxylin and eosin staining and immunohistochemistry of the lung tissue sections

Formalin-fixed and paraffin-embedded lung tissues were deparaffinized and cut into 4-μm-thick sections. Hematoxylin and eosin staining was performed by staining the nuclei with alum hematoxylin, differentiating with 0.3% acid alcohol, and staining with eosin for 2 min. The immunohistochemical staining was carried out as per the manufacturer's instructions (Boster, Wuhan China).

Cell transfection

The target sequences used to knock down Derlin-1 are shown in **Table 1**. The Derlin-1 and

the negative control small interfering RNA (siRNA) were provided by Shanghai Genechem Co., Ltd. (Shanghai, China). One day before the transfection, RLE-6TN cells were transferred into a 12-well plate at a density of 1×10^5 cells/well. The best Derlin-1 gene coding sequence was constructed into a lentiviral vector. This procedure was completed by Shanghai Genechem Co., Ltd. The RLE-6TN cells were cultured in a 12-well cultural plate to 30% confluency, and then 20 μL of 1×10^8 TU/mL virus was added.

After transfection with siRNA2 and lentivirus for two days, the samples with a transfection rate over 80% as assessed by fluorescence microscopy were selected for further experiments, and 10% CSE was added to each group for 3 h, 6 h, 12 h, and 24 h. Samples without CSE stimulation were designated as the 0 h group and the pcDNA5 empty vector was used as a negative control.

Apoptotic rate measured using flow cytometry

The cells were seeded in 6-well plates, grown to a 70% confluency, and transfected with an empty control siRNA or siRNA against Derlin-1. After incubation for 48 h, 2 mL of the medium containing 10% CSE was added. The cells were cultivated in a 5% CO_2 incubator at 37°C for 0 h, 3 h, 6 h, 12 h, and 24 h, then digested with trypsin without EDTA and suspended with 400 μL of binding buffer. After that, the cells were mixed with 5 μL of annexin V-FITC and 5 μL of propidium iodide and kept for 10 min at room temperature in the dark. The apoptotic rate was measured using flow cytometry (Beckman Coulter).

Quantitative real-time PCR

SYBR Green Main Mix (Dongsheng Biotechnology Co., Ltd., Guangzhou, China) and the Piko-Real 96 Real-time PCR System (Eppendorf, Hamburg, Germany) were used to perform real-time PCR. β-Actin was chosen as the reference gene. The relative target genes expressions were calculated using the 2-ΔΔCt method. The gene sequence was found in the NCBI database. The primer sequence was synthesized using Primer5 software (GenScript, Nanjing, China) as follows: Derlin-1-F, 5'-CATCCTGCGTCTGGACCTGG-3'; Derlin-1-R, 5'-TAATGTCACGCACGATTTCC-3'; β-actin-F, 5'-GGAACTGGATTTCTTTATTTG-3'; β-actin-R, 5'-TCTGACATGATCAGAGGAA-3'.

Western blot analysis

The total protein was extracted from the cells using a RIPA lysis buffer and quantified using the Bradford method. The protein samples were separated using sodium dodecyl sulfate-polyacrylamide gel electrophoresis and transferred to polyvinylidene fluoride membranes (Millipore, San Francisco, CA) and incubated at 4°C with primary antibodies at a specific dilution ratio (Derlin-1, 1:200; CHOP, 1:500; inositol requiring enzyme-1 (IRE1), p-IRE1, and JNK, 1:1000; and β-actin and p-JNK, 1:2000), followed by incubation with a horseradish peroxidase-conjugated secondary antibody (1:2000) at 37°C for two hours. The target protein on the polyvinylidene fluoride membrane was visualized using an electrochemiluminescence kit (Pierce, Rockford, IL) and obtained using the GIS-2010 imaging system (DNR Bio-Imaging Systems, Shanghai, China).

Statistical analysis

SPSS 18.0 software (SPSS Inc., Chicago, IL) was used for the statistical analysis. The results are shown as the mean ± standard deviation. If the data met the conditions of the parametric testing, one-way analyses of variance were used for the comparisons between groups and Newman-Keuls tests were used for the pairwise comparisons. Otherwise, an approximate t-test was used for the two independent samples. If $P < 0.05$, the difference was considered statistically significant.

Results

The Derlin-1 expression was significantly up-regulated in the COPD rats

As shown in **Figure 1**, smoking group 1 (2 months' exposure) had a lung tissue structure disorder with infiltrated lymphocyte-based inflammatory cells in the bronchial lungs and a partially-ruptured alveolar tissue structure. Smoking group 2 (4 months' exposure) had more severe tissue damage with a large amount of inflammatory cell infiltration in the bronchial lungs and ruptured alveolar walls fused into lung bullae. The pathologic findings and

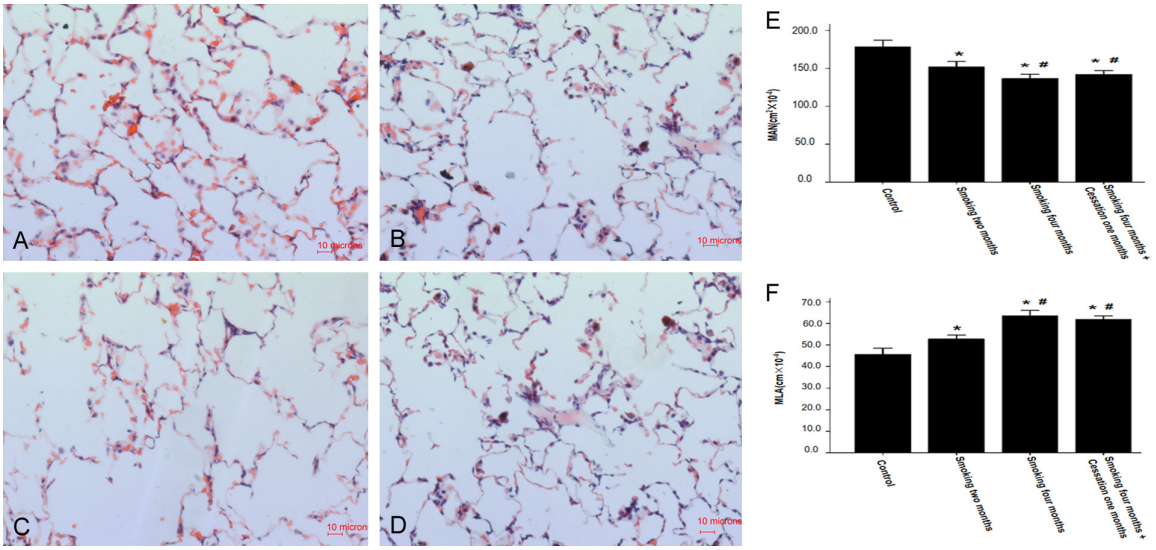

Figure 1. Results of the H&E staining on the lung tissue sections in the control group (A), smoking group 1 (B), smoking group 2 (C), and the smoking cessation group (D). Comparison of lung pulmonary mean alveolar number (MAN) among the different groups (E). Comparison of the lung pulmonary mean linear intercept number (MLA) among the different groups (F). *P < 0.05 vs the control group, # vs the smoking group 1.

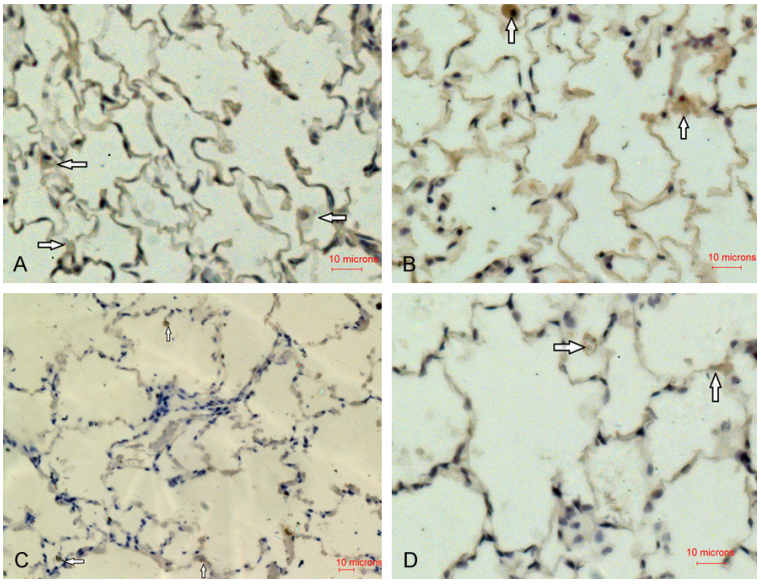

Figure 2. Immunohistochemical staining of Derlin-1 in the lung tissues in the different groups. Control group (A), smoking group 1 (B), smoking group 2 (C), and smoking cessation group (D). The white arrow indicates Derlin-1 expression.

functional test indicated that we successfully constructed the COPD rat model. The Derlin-1 protein was mainly expressed in the cytoplasms of the alveolar epithelial, bronchial epithelial, and vascular endothelial cells under a lighted microscope (**Figure 2**). The Derlin-1 mRNA and protein expressions in the smoking group were higher than they were in the control group (P < 0.05), and the expressions were higher in smoking group 1 than they were in smoking group 2 and the smoking cessation group (P < 0.05; **Figure 3A**, **3B**). The lung functions of the rats in the smoking groups and smoking cessation group were significantly lower than they were in the non-smoking control group (group 1: P < 0.05; group 2: P < 0.01, **Figure 3C**, **3D**). Although the smoking cessation group was slightly improved, there was no significant difference between the smoking group and the smoking cessation group (P > 0.05; **Figure 3C**, **3D**). The Derlin-1 mRNA and Derlin-1 protein expressions in the RLE-6TN cells treated with CSE increased at first but then decreased, with the expressions highest at 6 h (P < 0.05, **Figure 4A**, **4B**).

Derlin-1 siRNA effectively silenced and lentivirus overexpression Derlin-1 in RLE-6TN cells

As shown in **Figure 5**, the expression of the Derlin-1 protein in the RLE-6TN cells after the

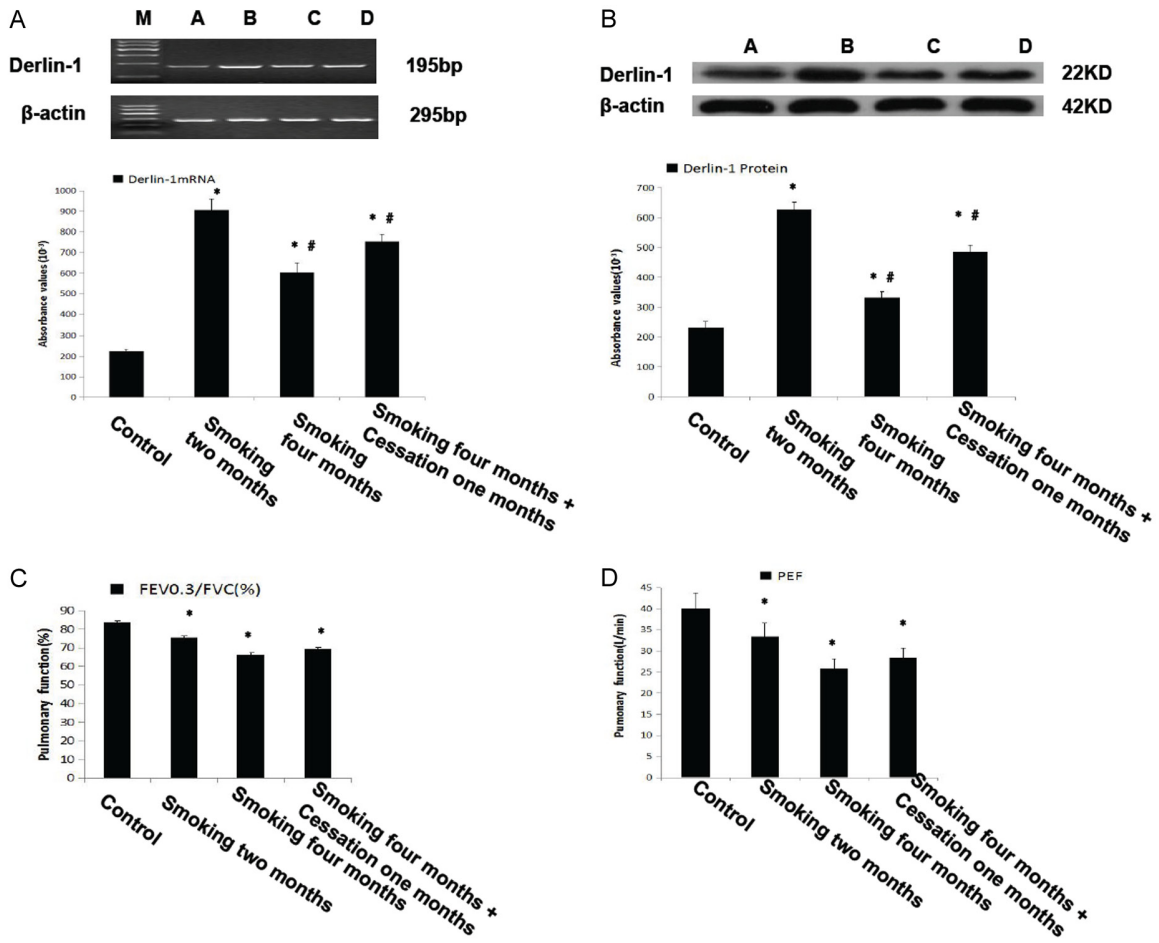

Figure 3. Comparisons among the different rat groups. Derlin-1 mRNA (A). Derlin-1 protein (B) and $FEV_{0.3}$/FVC (%) (C), PEF (L/min) (D). **P* < 0.05 vs the control group, #*P* < 0.05 vs smoking group 1.

siRNA2 transfection was significantly lower in the silence group than in the empty group (*P* < 0.05). The expression of the Derlin-1 protein was significantly higher in the lentivirus-transfected group of RLE-6TN cells than it was in the empty group (*P* < 0.05; **Figure 6**).

Apoptotic rate measured using flow cytometry

We speculated that Derlin-1-induced apoptosis might be associated with COPD. Therefore, we knocked down Derlin-1 expression and stimulated the RLE-6TN cell lines with CSE to mimic smoking induction. The apoptotic rates of the cells treated with CSE at different times were evaluated using flow cytometry at different time points. As shown in **Figure 7**, with the prolongation of the 10% CSE stimulation time, the apoptotic rate of the Derlin-1 silence group was significantly higher than the corresponding rate in the empty group (*P* < 0.05), and the apoptotic rate of the over-expression group was significantly lower than the apoptotic rate in the empty group (*P* < 0.05; **Figure 7**).

Change in the Derlin-1 expression after CSE exposure in cells with silenced and over-expressed Derlin-1

Compared with the steadily increased expression of Derlin-1 mRNA in the empty group, the expression of Derlin-1 mRNA in the silence group showed no significant change at 3 h or 6 h (*P* > 0.05) and was significantly increased at 12 h and 24 h (*P* < 0.05; **Figure 7A**). The expression of Derlin-1 in the over-expression group was increased with the dose amount of stimulus. The different time groups showed significant differences (*P* < 0.05), and the expression of Derlin-1 in the over-expression group was significantly higher than it was in the empty group at 12 h and 24 h (*P* < 0.05; **Figure 7D**).

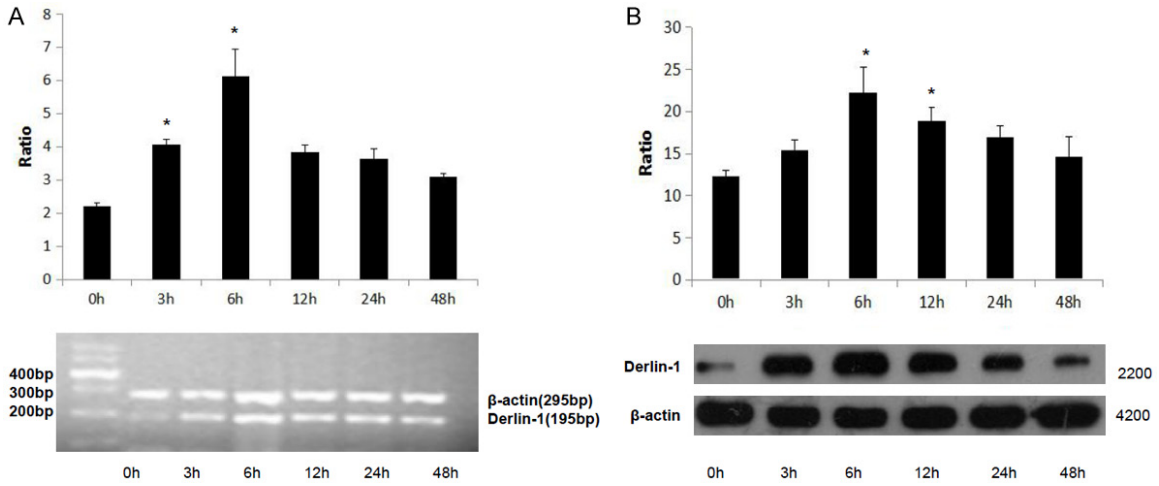

Figure 4. Change in the expression of Derlin-1 in the RLE-6TN cells treated with 10% CSE. *P < 0.05 vs the control group.

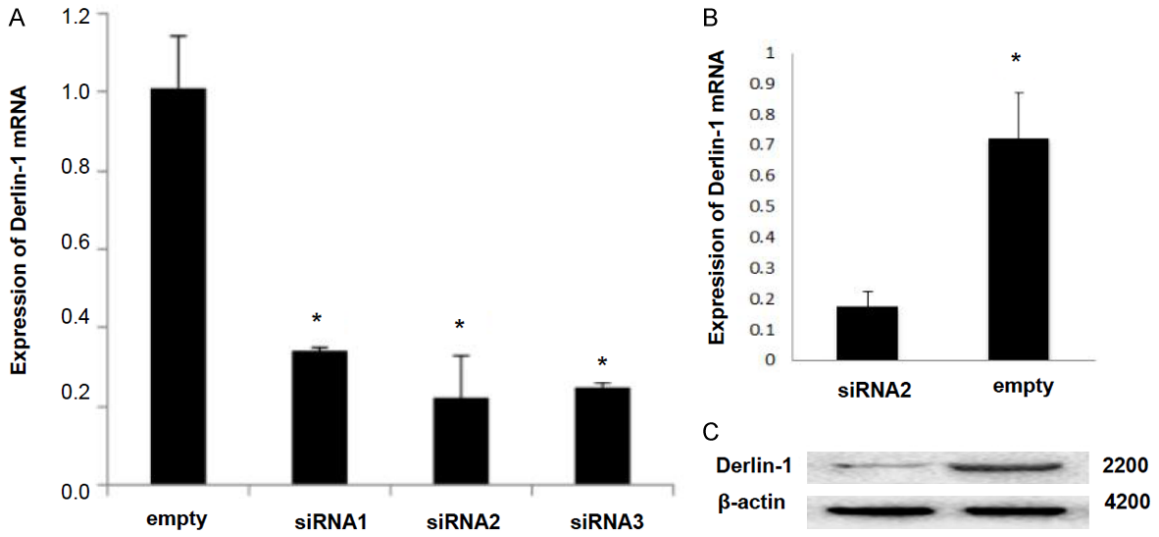

Figure 5. The Derlin-1 mRNA (A) and protein expressions (B and C) in the RLE-6TN cells transfected with siRNA. *P < 0.05 vs the empty group.

The RT-PCR results were consistent with the western blot results (**Figure 8**).

Effects of Derlin-1 gene expression intervention on the total protein and phosphorylation of IRE1 and p-IRE1 in RLE-6TN induced by CSE

In order to determine whether the Derlin-1-related ERS is UPR signaling pathway-dependent, we measured the IRE1 and p-IRE1 expressions after silencing and over-expressing Derlin-1 in the RLE-6TN cell lines. As shown in **Tables 2** and **3**, there were no significant differences in the IRE1 total protein expressions in the empty, silence, and over-expression groups at each time point (P > 0.05). The p-IRE1 expressions in the empty and over-expression groups were increased with the prolongation of the CSE exposure time, and significant differences existed between the two groups at different time points (P < 0.05). In the silence group, the expression of the P-IRE1 protein was up-regulated at 3 h, 6 h, and 12 h. There was no significant difference at 24 h (P > 0.05). In the over-expression groups, P-IRE1 gradually increased with time, but the P-IRE1 levels in both groups were lower than the P-IRE1 level in the empty group (P < 0.05).

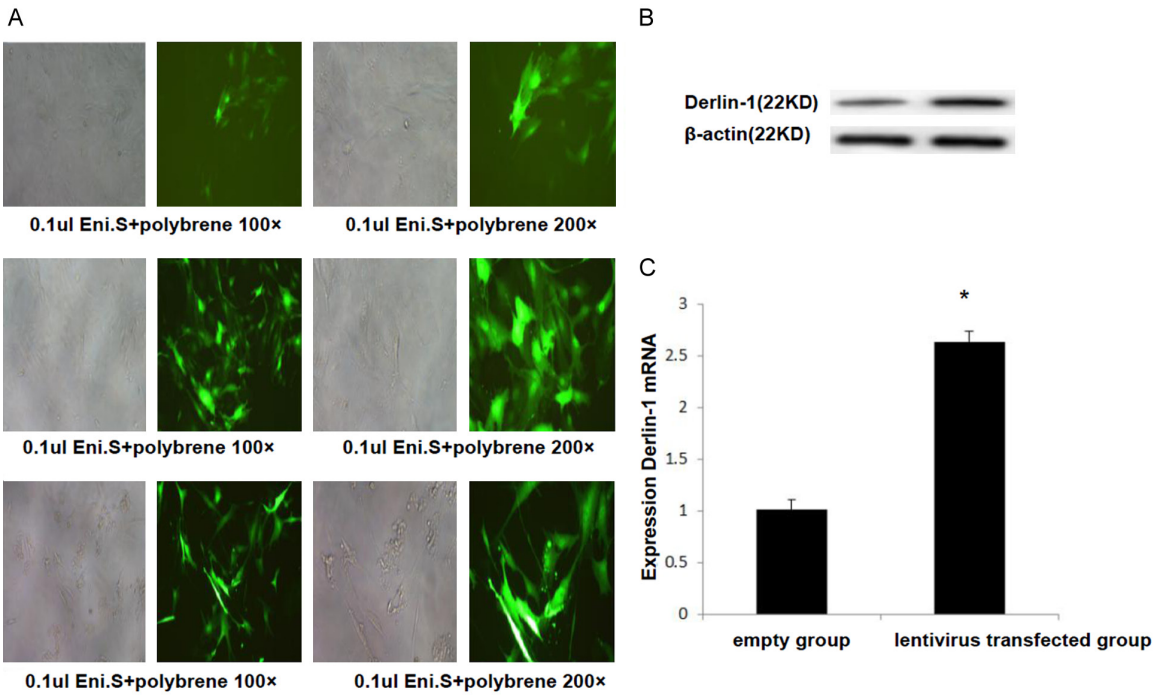

Figure 6. Evaluation of transfection efficiency of the RLE-6TN cells treated by lentivirus (A). The Derlin-1 mRNA (B) and protein (C) expressions in the RLE-6TN cells transfected using lentivirus. *$P < 0.05$ vs the empty group.

Effects of the Derlin-1 gene expression intervention on the total protein and phosphorylation of JNK, p-JNK, and CHOP

We showed that Derlin-1 significantly down-regulated ERS-related apoptosis in COPD. Because p-JNK and CHOP mediate ERS-related apoptosis, we studied whether Derlin-1 associated with COPD apoptosis was related to p-JNK and CHOP. The JNK total protein expressions were not different in the empty, silence, and over-expression groups at each time point ($P > 0.05$). The p-JNK and CHOP expressions in the empty and over-expression groups were increased with longer CSE exposure times, and significant differences existed between the two groups at the different time points ($P < 0.05$). The CHOP and p-JNK protein expressions were higher in the silence group than in the empty group ($P < 0.05$), and the CHOP and p-JNK protein expressions were lower in the over-expression group than they were in the empty group ($P < 0.05$; **Tables 2** and **3**).

Discussion

When considering how ER stress affects the pathogenesis of a disease, most studies have focused on ER stress-induced apoptosis. More and more evidence suggests that smoking-induced pulmonary epithelial cell apoptosis plays an important role in the pathogenesis of COPD emphysema [1, 3]. Based on a proteomics study conducted in 2008, Kelsen et al. [8] reported that smoking can cause ERS and up-regulate glucose-regulated protein 78 (GRP78) expression in bronchial epithelial cells. He et al. [16] tested the GRP78, CHOP, and caspase-12 levels and the apoptosis rate of rat alveolar epithelial cells in a rat model of smoking COPD, showing that ERS is an important way to mediate the apoptosis of alveolar epithelial cells and concluding that ERS-mediated alveolar epithelial apoptosis may be one of COPD's mechanisms. Our previous study [6] showed that CSE induces ERS in lung epithelial cells, subsequently leading to lung injury in rats, so it may be a new target for the ER endothelial cell protection of emphysema. We showed that as exposure to cigarette smoke was prolonged in the smoking COPD rat model, the alveolar walls ruptured and gradually fused into pulmonary bullae. Although lung inflammation in the smoking cessation group was significantly reduced, the development of emphysema was observed and the change in pulmonary function satisfied the diagnostic criteria for

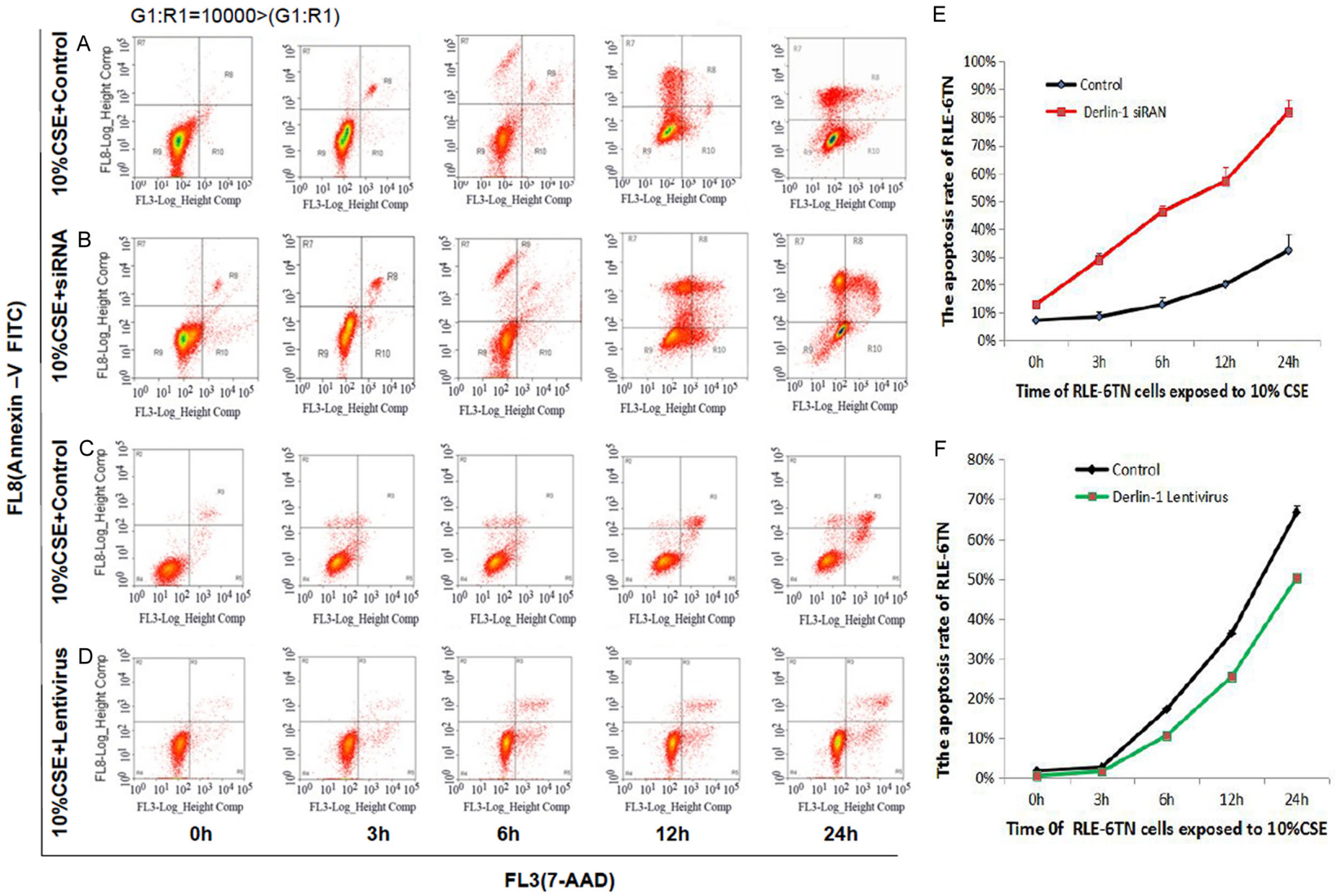

Figure 7. Annexin V⁺ apoptotic rate measured using flow cytometry in the empty (A), silence (B), control (C), and over-expression Derlin-1 mRNA groups (D). The annexin V⁺ apoptotic rate of the RLE-6TN cells for the empty and silence groups exposed to 10% CSE at different time points (E). Annexin V⁺ apoptotic rate of the RLE-6TN cells for the empty and Derlin-1 over-expression groups exposed to 10% CSE at different time points (F).

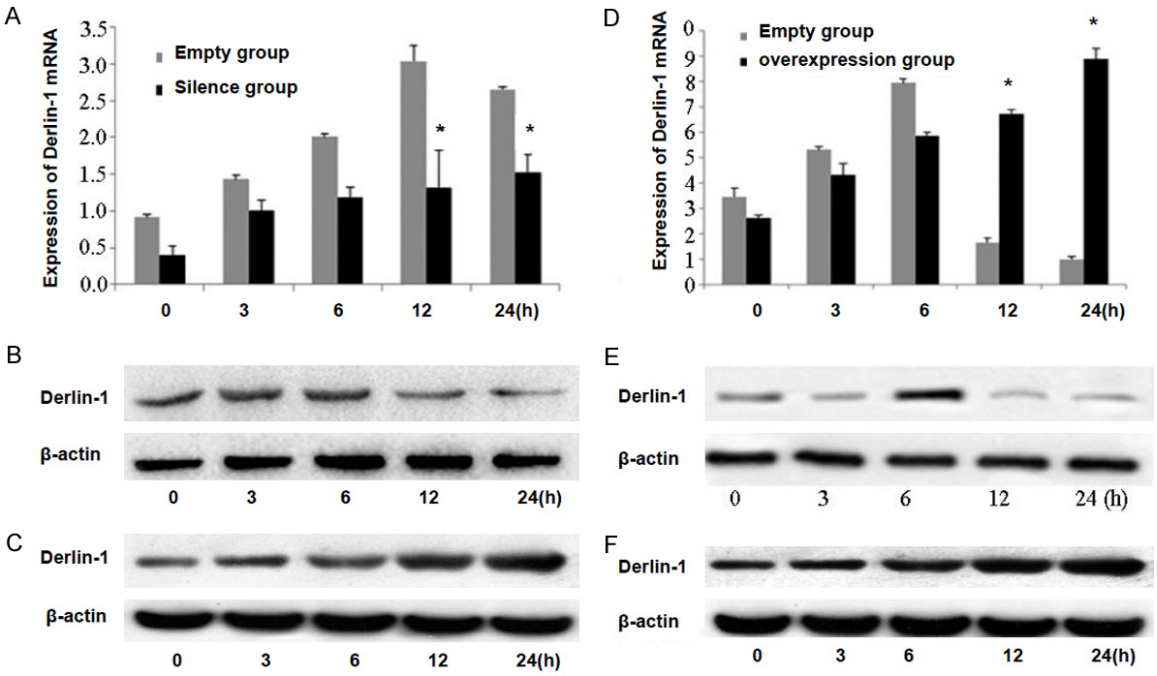

Figure 8. The Derlin-1 mRNA expression in RLE-6TN measured using RT-PCR (A and D). The Derlin-1 protein expression in the RLE-6TN cells measured using western blot in the no-load plasmid set control (B), Derlin-1 silence (C), no-load lentivirus control (E), and Derlin-1 over-expression groups (F). *$P < 0.05$ vs the empty group.

Table 2. The P-IRE-1, P-JNK, and CHOP protein expressions in the empty and silence groups with different treatment durations

Time	Empty group					Silence group				
	IRE1	P-IRE1	JNK	P-JNK	CHOP	IRE1	P-IRE1	JNK	P-JNK	CHOP
0 h	1.51±0.34	0.95±0.01	0.97±0.07	0.29±0.02	1.32±0.40	1.52±0.14	0.33±0.02	0.87±0.24	0.22±0.01	0.41±0.06
3 h	1.84±0.34	1.62±0.02	0.94±0.11	0.66±0.02	2.92±0.50	1.23±0.11	0.48±0.02	0.65±0.031	0.46±0.07	0.80±0.08
6 h	1.91±0.36	2.26±0.03	1.11±0.06	0.63±0.01	4.53±0.60	1.24±0.15	0.84±0.04	0.85±0.15	0.64±0.08	1.70±0.19
12 h	1.93±0.32	7.13±0.31	1.05±0.04	0.60±0.11	10.54±1.04	1.28±0.19	0.36±0.01	0.82±0.033	0.24±0.03	1.99±0.21
24 h	1.82±0.35	9.12±0.20	1.12±0.09	0.71±0.15	9.01±1.4	1.21±0.15	0.32±0.03	0.872±0.19	0.28±0.04	1.60±0.19
F	0.737	1466.52	3.252	11.649	76.745	2.172	210.794	1.096	34.662	52.5
P	0.588	< 0.001	0.059	< 0.001	< 0.001	0.146	< 0.001	0.41	< 0.001	< 0.001

Table 3. The P-IRE-1, P-JNK, and CHOP protein expressions in the empty and overexpression groups with different treatment durations

Time	Empty group					Overexpression group				
	IRE1	P-IRE1	JNK	P-JNK	CHOP	IRE1	P-IRE1	JNK	P-JNK	CHOP
0 h	0.50±0.01	0.22±0.01	0.61±0.02	0.21±0.01	0.40±0.02	0.37±0.02	0.13±0.01	0.24±0.02	0.15±0.01	0.21±0.02
3 h	0.52±0.02	0.25±0.01	0.59±0.01	0.34±0.02	0.54±0.02	0.36±0.01	0.14±0.01	0.22±0.02	0.17±0.01	0.28±0.01
6 h	0.52±0.02	0.30±0.01	0.59±0.02	0.43±0.01	0.66±0.01	0.35±0.02	0.20±0.02	0.24±0.01	0.23±0.01	0.34±0.01
12 h	0.54±0.02	0.40±0.01	0.58±0.02	0.65±0.02	0.85±0.01	0.34±0.00	0.29±0.01	0.20±0.02	0.33±0.02	0.44±0.01
24 h	0.51±0.02	0.44±0.01	0.59±0.02	0.78±0.02	0.96±0.01	0.35±0.01	0.35±0.02	0.23±0.03	0.40±0.01	0.52±0.01
F	3.068	382.182	0.741	717.472	729.141	2.929	237.452	1.932	286.944	374.553
P	0.069	< 0.001	0.585	< 0.001	< 0.001	0.077	< 0.001	0.182	< 0.001	< 0.001

COPD. In the cell experiments, following treatment of RLE-6TN cells with 10% CSE, the CHOP and JNK expressions, as well as the apoptotic rate, were increased with the prolongation of CSE exposure time. Thus, it was confirmed that CSE-mediated ERS leads to apoptosis in RLE-6TN cells. This finding provides support for the notion that the stress-induced apoptosis of

alveolar type II epithelial cells is caused by CSE and therefore participates in the mechanism underlying COPD.

Recently, Sekiya et al. [19] reported that ERS promotes the up-regulation of degradation errors and unfolded proteins using the ERAD pathway-associated protein EDEM function. In our study, Derlin-1 expression was up-regulated in the lung tissue of smoke-exposed rats, but the Derlin-1 expressions in the rat lung tissues in the smoking group 1 and the smoking cessation group gradually decreased. Thus, the Derlin-1 expressions were significantly correlated with the time and quantity of CSE; however, this did not show whether Derlin-1 plays a role in anti-apoptosis. Our results were further validated by the primary type II alveolar epithelial and RLE-6TN cells stimulated with CSE. The results showed that the Derlin-1 protein and mRNA levels were increased, but then decreased, which is consistent with the results of the animal experiments. Through gene in -1 expression was down-regulated and decreased when Derlin-1 expression was up-regulated. The up-regulated expression of Derlin-1 was limited; thus, with the increase in smoke exposure time and number, Derlin-1 did not increase and showed a downward trend. This is consistent with the role of the ERAD pathway in the UPR [2, 23]. If ERAD and other aspects of the UPR are unable to address ER stress, the maladaptive features of the UPR lead to apoptosis, which contributes to the tissue damage and organ dysfunction [18, 25]. When the Derlin-1 gene expression is down-regulated, the ER11 pathway is inhibited and apoptosis is accelerated. Conversely, the apoptotic rate in the Derlin-1 over-expression group was significantly reduced. These findings suggest that Derlin-1 may increase the chemical resistance of alveolar epithelial cells by accelerating ERAD and may play a role in CSE-induced COPD.

In the event of ERS, the sequential order of activation of the UPR signaling pathway is from the early PERK and ATF6 to the late IRE1 [27]. The IRE1 pathway is mainly characterized by cell adaptation and increased protein folding [11, 15, 24], but the activation of the PERK and ATF6 pathways leads to elevated levels of the pro-apoptotic components. Thus, the IRE1 pathway is particularly important for this protective response [13]. IREl/X-box binding protein 1 promotes the elimination of the retention protein in ER by the up-regulated expression of genes, such as EDEM and Derlin-1 [10]. Activated IRE1 also up-regulates the expression of CHOP and induces cell apoptosis by modulating the apoptosis signal-regulating kinase 1-JNK signaling pathway [7]. The final outcome is that cell survival or death depends on the balance of power between the survival signal and the death signal [16]. By examining the IRE1, CHOP, and JNK protein expressions before and after the intervention of the Derlin-1 gene, we preliminarily verified the expression of Derlin-1 in the ERAD pathway. Our results show that the increased expression change of Derlin-1 is negative feedback regulation of IRE1 to promote cell survival or apoptosis, indicating that Derlin-1 is not only involved in material transport and identification, but it also may be involved in ERAD pathway regulation.

Conclusion

In conclusion, this study showed that CSE can induce alveolar epithelial cell apoptosis through the ERS mechanism, and the over-expression of Derlin-1 shows an anti-apoptotic effect, suggesting that Derlin-1 may be an important factor involved in regulating the physiologic function of alveolar epithelial cells. An in-depth study on the role of Derlin-1 in the ERAD pathway and the underlying mechanism could help increase our understanding of the mechanism of the body's resistance to cigarette smoke-induced alveolar epithelial cell apoptosis and provide new strategies for the treatment of COPD.

Acknowledgements

The animal experiments were approved by the Institutional Review Board of our hospital and carried out in accordance with the Declaration of Helsinki. This study was supported by a grant from the National Natural Science Foundation of China (No. 81070035).

Disclosure of conflict of interest

None.

Address correspondence to: Dr. Rui-Cheng Hu, Department of Respiratory Medicine, Hunan Provincial People's Hospital/The First Affiliated Hospital of Hunan Normal University, 89 Guhan Road, Chang-

sha 410016, Hunan, China. E-mail: huruicheng@hotmail.com

References

[1] Zong D, Li J, Cai S, He S, Liu Q, Jiang J, Chen S, Long Y, Chen Y, Chen P and Ouyang R. Notch1 regulates endothelial apoptosis via the ERK pathway in chronic obstructive pulmonary disease. Am J Physiol Cell Physiol 2018; 315: C330-C340.

[2] Claessen JH, Kundrat L and Ploegh HL. Protein quality control in the ER: balancing the ubiquitin chequebook. Trends Cell Biol 2012; 22: 22-32.

[3] Chambers E, Rounds S and Lu Q. Pulmonary endothelial cell apoptosis in emphysema and acute lung injury. Adv Anat Embryol Cell Biol 2018; 228: 63-86.

[4] Dong Q, Fu L, Zhao Y, Tan S and Wang E. Derlin-1 overexpression confers poor prognosis in muscle invasive bladder cancer and contributes to chemoresistance and invasion through PI3K/AKT and ERK/MMP signaling. Oncotarget 2017; 8: 17059-17069.

[5] Dong QZ, Wang Y, Tang ZP, Fu L, Li QC, Wang ED and Wang EH. Derlin-1 is overexpressed in non-small cell lung cancer and promotes cancer cell invasion via EGFR-ERK-mediated up-regulation of MMP-2 and MMP-9. Am J Pathol 2013; 182: 954-964.

[6] Gan G, Hu R, Dai A, Tan S, Ouyang Q, Fu D and Jiang D. The role of endoplasmic reticulum stress in emphysema results from cigarette smoke exposure. Cell Physiol Biochem 2011; 28: 725-732.

[7] Yi S, Chen K, Zhang L, Shi W, Zhang Y, Niu S, Jia M, Cong B and Li Y. Endoplasmic reticulum stress is involved in stress-induced hypothalamic neuronal injury in rats via the PERK-ATF4-CHOP and IRE1-ASK1-JNK pathways. Cigarette smoke extract induces endothelial cell injury via JNK pathway. Front Cell Neurosci 2019; 13: 190.

[8] Kelsen SG, Duan X, Ji R, Perez O, Liu C and Merali S. Cigarette smoke induces an unfolded protein response in the human lung: a proteomic approach. Am J Respir Cell Mol Biol 2008; 38: 541-550.

[9] Hano M, Tomášová L, Šereš M, Pavlíková L, Breier A and Sulová Z. Interplay between P-glycoprotein expression and resistance to endoplasmic reticulum stressors. Molecules 2018; 23: 337.

[10] Guiliano DB, Fussell H, Lenart I, Tsao E, Nesbeth D, Fletcher AJ, Campbell EC, Yousaf N, Williams S, Santos S, Cameron A, Towers GJ, Kellam P, Hebert DN, Gould KG, Powis SJ and Antoniou AN. Endoplasmic reticulum degradation-enhancing α-mannosidase-like protein 1 targets misfolded HLA-B27 dimers for endoplasmic reticulum-associated degradation. Arthritis Rheumatol 2014; 66: 2976-88.

[11] Lhomond S, Pallares N, Barroso K, Schmit K, Dejeans N, Fazli H, Taouji S, Patterson JB and Chevet E. Adaptation of the secretory pathway in cancer through IRE1 signaling. Methods Mol Biol 2015; 1292: 177-194.

[12] Lilley BN and Ploegh HL. A membrane protein required for dislocation of misfolded proteins from the ER. Nature 2004; 429: 834-840.

[13] Tsuchiya Y, Saito M, Kadokura H, Miyazaki JI, Tashiro F, Imagawa Y, Iwawaki T and Kohno K. IRE1-XBP1 pathway regulates oxidative proinsulin folding in pancreatic β cells. J Cell Biol 2018; 217: 1287-1301.

[14] Mouded M, Egea EE, Brown MJ, Hanlon SM, Houghton MG, Tsai LW, Ingenito EP and Shapiro SD. Epithelial cell apoptosis causes acute lung injury masquerading as emphysema. Am J Respir Cell Mol Biol 2009; 41: 407-414.

[15] Adams CJ, Kopp MC, Larburu N, Nowak PR and Ali MMU. Structure and molecular mechanism of ER stress signaling by the unfolded protein response signal activator IRE1. Front Mol Biosci 2019; 6: 11.

[16] Oono K, Yoneda T, Manabe T, Yamagishi S, Matsuda S, Hitomi J, Miyata S, Mizuno T, Imaizumi K, Katayama T and Tohyama M. JAB1 participates in unfolded protein responses by association and dissociation with IRE1. Neurochem Int 2004; 45: 765-772.

[17] Pi L, Zhu G, She L, Wei M, Liu G, Chen C, Hu D, Peng F, Tan H, Liu Y, Huang D, Tian Y and Zhang X. Elevated expression of Derlin-1 associates with unfavorable survival time of squamous cell carcinoma of the head and neck and promotes its malignance. J Cancer 2017; 8: 2336-2345.

[18] Sano R and Reed JC. ER stress-induced cell death mechanisms. Biochim Biophys Acta 2013; 1833: 3460-3470.

[19] Sekiya M, Maruko-Otake A, Hearn S, Sakakibara Y, Fujisaki N, Suzuki E, Ando K and Iijima KM. EDEM function in ERAD protects against chronic ER proteinopathy and age-related physiological decline in drosophila. Dev Cell 2017; 41: 652-664.

[20] Tan X, He X, Jiang Z, Wang X, Ma L, Liu L, Wang X, Fan Z and Su D. Derlin-1 is overexpressed in human colon cancer and promotes cancer cell proliferation. Mol Cell Biochem 2015; 408: 205-213.

[21] Vayssiertaussat M, Camilli T, Aron Y, Meplan C, Hainaut P, Polla BS and Weksler B. Effects of tobacco smoke and benzo[a]pyrene on human endothelial cell and monocyte stress respons-

es. Am J Physiol Heart Circ Physiol 2001; 280: H1293-H1300.
[22] Vogelmeier CF, Criner GJ, Martinez FJ, Anzueto A, Barnes PJ, Bourbeau J, Celli BR, Chen R, Decramer M, Fabbri LM, Frith P, Halpin DM, López Varela MV, Nishimura M, Roche N, Rodriguez-Roisin R, Sin DD, Singh D, Stockley R, Vestbo J, Wedzicha JA and Agustí A. Global strategy for the diagnosis, management and prevention of chronic obstructive lung disease 2017 report. Am J Respir Crit Care Med 2017; 195: 557-582.
[23] Walter P and Ron D. The unfolded protein response: from stress pathway to homeostatic regulation. Science 2011; 334: 1081-1086.
[24] Wu J, He GT, Zhang WJ, Xu J and Huang QB. IRE1α signaling pathways involved in mammalian cell fate determination. Cell Physiol Biochem 2016; 38: 847-858.
[25] Kapuy O, Márton M, Bánhegyi G and Vinod PK. Multiple system-level feedback loops control life-and-death decisions in endoplasmic reticulum stress. FEBS Lett 2020; 594: 1112-1123.
[26] Ye Y, Shibata Y, Yun C, Ron D and Rapoport TA. A membrane protein complex mediates retrotranslocation from the ER lumen into the cytosol. Nature 2004; 429: 841-847.
[27] Yoshida H, Matsui T, Hosokawa N, Kaufman RJ, Nagata K and Mori K. A time-dependent phase shift in the mammalian unfolded protein response. Dev Cell 2003; 4: 265-271.